Central chemoreceptors and sympathetic vasomotor outflow

Thiago S. Moreira[1,2], Ana C. Takakura[1,2], Eduardo Colombari[2] and Patrice G. Guyenet[1]

[1]*Department of Pharmacology, University of Virginia, Charlottesville, VA, 22908, USA*
[2]*Department of Physiology, UNIFESP-EPM, São Paulo, SP, 04023-060, Brazil*

The present study explores how elevations in brain P_{CO_2} increase the sympathetic nerve discharge (SND). SND, phrenic nerve discharge (PND) and putative sympathoexcitatory vasomotor neurons of the rostral ventrolateral medulla (RVLM) were recorded in anaesthetized sino-aortic denervated and vagotomized rats. Hypercapnia (end-expiratory CO_2 from 5% to 10%) increased SND (97 ± 6%) and the activity of RVLM neurons (67 ± 4%). Injection of kynurenic acid (Kyn, ionotropic glutamate receptor antagonist) into RVLM or the retrotrapezoid nucleus (RTN) eliminated or reduced PND, respectively, but did not change the effect of CO_2 on SND. Bilateral injection of Kyn or muscimol into the rostral ventral respiratory group (rVRG-pre-Bötzinger region, also called CVLM) eliminated PND while increasing the stimulatory effect of CO_2 on SND. Muscimol injection into commissural part of the solitary tract nucleus (commNTS) had no effect on PND or SND activation by CO_2. As expected, injection of Kyn into RVLM or muscimol into commNTS virtually blocked the effect of carotid body stimulation on SND in rats with intact carotid sinus nerves. In conclusion, CO_2 increases SND by activating RVLM sympathoexcitatory neurons. The relevant central chemoreceptors are probably located within or close to RVLM and not in the NTS or in the rVRG-pre-Bötzinger/CVLM region. RVLM sympathoexcitatory neurons may be intrinsically pH-sensitive and/or receive excitatory synaptic inputs from RTN chemoreceptors. Activation of the central respiratory network reduces the overall sympathetic response to CO_2, presumably by activating barosensitive CVLM neurons and inhibiting RTN chemoreceptors.

(Received 19 June 2006; accepted after revision 7 August 2006; first published online 10 August 2006)
Corresponding author P. G. Guyenet: Department of Pharmacology, University of Virginia Health System, PO Box 800735, 1300 Jefferson Park Avenue, Charlottesville, VA 22908-0735, USA. Email: pgg@virginia.edu

In the absence of input from carotid bodies and cardiopulmonary receptors hypercapnia markedly increases sympathetic nerve discharge (SND) to the heart and blood vessels (Hanna *et al.* 1988). The effect of CO_2 is generally attributed to the following chain of events: brain extracellular fluid acidification stimulates central 'respiratory' chemoreceptors, these chemoreceptors activate the respiratory pattern generator (CPG) and the CPG ultimately drives the sympathetic generating network by phasically exciting the sympathoexcitatory neurons of the rostral ventrolateral medulla (RVLM) (Millhorn & Eldridge, 1986; Richter & Spyer, 1990; Guyenet & Koshiya, 1992). This theory relies on the following evidence. SND activation by central chemoreceptors occurs in bursts that are synchronized with the central respiratory cycle (Millhorn, 1986; Millhorn & Eldridge, 1986; Guyenet *et al.* 1990; Habler *et al.* 1994). Damage to the ventrolateral medullary surface via cooling, lesions or chemicals typically attenuates PND and the respiratory oscillations of SND in roughly proportional manner (Hanna *et al.* 1979; Millhorn, 1986; Millhorn & Eldridge, 1986). During central chemoreceptor stimulation, RVLM sympathoexcitatory neurons exhibit patterns of central respiratory-related activity that are similar to those of barosensitive sympathetic ganglionic neurons (McAllen, 1987; Haselton & Guyenet, 1989; Darnall & Guyenet, 1990; Guyenet *et al.* 1990; Miyawaki *et al.* 1995).

However, a number of assumptions underlying the currently accepted view on how CO_2 affects SND have not been tested. For example, the proposed circuit presumes that the sympathetic generating network does not contain pH-responsive elements. Already challenged 25 years ago (Trzebski & Kubin, 1981), this premise is even less persuasive at present given recent evidence that the pontomedullary region may contain multiple sites for respiratory chemoreception (nucleus of the solitary

T. S. Moreira and A. C. Takakura contributed equally to this study.

 DOI: 10.1113/jphysiol.2006.115600

tract (NTS), retrotrapezoid nucleus (RTN), pre-Bötzinger complex, raphe) (Nattie & Li, 1996; Feldman *et al.* 2003; Hodges *et al.* 2004; Mulkey *et al.* 2004; Putnam *et al.* 2004; Richerson *et al.* 2005). Noradrenergic neurons are pH-sensitive (Pineda & Aghajanian, 1997) and RVLM sympathoexcitatory neurons may also have this property given that they express high levels of TASK channels, have close relationships with capillaries and possess dendrites that reach the ventral medullary surface (Milner *et al.* 1987, 1989; Washburn *et al.* 2003). Second, the observation that RVLM vasomotor neurons are respiratory rhythmic is insufficient to conclude that these cells cause the increased SND associated with central chemoreceptor stimulation. Only one study has examined whether the overall activity of these neurons is actually increased by central chemoreceptor stimulation (Haselton & Guyenet, 1989) and none has examined whether their degree of activation is commensurate with the rise in sympathetic vasomotor tone. Third, the fact that SND or RVLM neurons are activated in bursts during central chemoreceptor stimulation does not mean that such bursts are caused by respiratory rhythmic excitatory volleys to the RVLM neurons. Respiratory synchronous bursts can be sculpted by periodic inhibitory inputs from a background of tonic excitation. Many ventral respiratory group (VRG) expiratory neurons and the chemosensitive neurons of RTN derive their respiratory modulation in this fashion during central chemoreceptor stimulation (Sun *et al.* 2001; Guyenet *et al.* 2005*a*). The same type of synaptic mechanism could also account for the central respiratory modulation of RVLM neurons since their principal tonically active GABAergic input from caudal ventrolateral medulla (CVLM) neurons is strongly respiratory modulated (Schreihofer & Guyenet, 2003; Mandel & Schreihofer, 2006).

The goal of the present experiments is to test several of the unproven assumptions that underlie our present understanding of how central chemoreceptors activate vasomotor SND. The main objectives are to test rigorously the role of RVLM neurons in this reflex, to determine whether the activation of these cells relies on glutamate-mediated excitatory inputs and to circumscribe the region of the medulla oblongata which contains the pH-sensitive elements that are primarily responsible for elevating sympathetic vasomotor tone.

Methods

Animals

The experiments were performed on 68 male Sprague-Dawley rats (Taconic; Germantown, NY, USA) weighing 270–350 g. Procedures were in accordance with NIH Animal Care and Use Guidelines and were approved by the University of Virginia Animal Care and Use Committee.

Surgery and anaesthesia

General anaesthesia was induced with 5% halothane in 100% oxygen. The rats received a tracheostomy and surgery was done under artificial ventilation with 1.4–1.5% halothane in 100% oxygen. All rats were subjected to the following previously described surgical procedures: femoral artery cannulation for arterial pressure (AP) measurement, femoral vein cannulation for administration of fluids and drugs, removal of the occipital plate for insertion of a pipette for microinjection or insertion of a recording electrode into the medulla oblongata via a dorsal transcerebellar approach, and skin incision over the lower jaw for placement of a bipolar stimulating electrode next to the mandibular branch of the facial nerve (Guyenet *et al.* 2005*a*). The phrenic nerve was accessed by a dorsolateral approach after retraction of the right shoulder blade. All animals were bilaterally vagotomized to prevent entrainment of the phrenic nerve discharge to the ventilator. In most rats a complete baro- and peripheral chemoreceptor deafferentation was performed by sectioning the vagosympathetic trunks, the superior laryngeal nerves and the glossopharyngeal nerves (proximal to the junction with the carotid sinus nerves). In the others (baro- and chemo-receptor intact group), the vagus nerves were carefully separated from the vagosympathetic trunk and selectively transected bilaterally. We presume that this procedure left the aortic depressor nerves intact but these very fine nerves were not identified.

Splanchnic sympathetic nerve discharge (sSND) was recorded as previously described (Schreihofer & Guyenet, 2000*a*,*b*; Schreihofer *et al.* 2000). The right splanchnic nerve was isolated via a retroperitoneal approach, and the segment distal to the suprarenal ganglion was placed on a pair of Teflon-coated silver wires that had been bared at the tip (250 μm bare diameter; A-M Systems, www.a-msystems.com). In some experiments, lumbar sympathetic nerve discharge (lSND) was also recorded as previously described (Haselton & Guyenet, 1989; Guyenet *et al.* 1990). In this case a ventral approach to the sympathetic chain was used. The nerves and wires were embedded in dental impression material (polyvinylsiloxane; Darby.Spencer.Mead Dental Supply, www.darbyspencermead.com), and the incision site was closed around the exiting recording wires.

Upon completion of surgical procedures, halothane concentration was adjusted (0.9–1%) for each animal to a level sufficient to abolish the corneal reflex and the retraction of distal phalanges to strong nociceptive stimulation of the hindpaw. Since halothane has a marked depressant effect on carotid body function, urethane was used in experiments requiring preservation of the peripheral chemoreflex. Thus, in the rats with intact baro- and chemoreceptors, after completion of surgical procedures, halothane was replaced by urethane

(1.2–1.5 g kg^{-1}) administered slowly I.V. All rats were ventilated with 100% oxygen throughout the experiment. Rectal temperature (maintained at 37°C) and end tidal-CO_2 were monitored throughout the experiment with a capnometer (Columbus Instruments, Ohio, USA) that was calibrated twice per experiment against a calibrated CO_2–N_2 mix. This instrument provided a reading of $< 0.1\%$ CO_2 during inspiration in animals breathing 100% oxygen and an asymptotic, nearly horizontal reading during expiration. We previously showed that the capnometer readings closely approximate arterial P_{CO_2} (Guyenet *et al.* 2005*a*). Regardless of the anaesthetic used, the adequacy of anaesthesia was monitored during a 20 min stabilization period by testing for absence of withdrawal response, lack of AP change and lack of change in PND rate or amplitude to firm toe pinch. After these criteria were satisfied, the neuromuscular blocker pancuronium was administered at the initial dose of 1 mg kg^{-1} I.V. and the adequacy of anaesthesia was thereafter gauged solely by the lack of increase in AP and PND rate or amplitude to firm toe pinch. No adjustment of the halothane concentration was needed. However, approximately hourly supplements of one-third of the initial dose of urethane were needed to satisfy these criteria during the course of the recording period (4 h).

In vivo recordings of physiological variables and neuronal activity

Arterial pressure (AP), the mass discharge of the phrenic (PND), splanchnic (sSND) and lumbar (lSND) nerves, tracheal CO_2 and single units were recorded as previously described (Guyenet *et al.* 2005*a*).

As in prior work, the caudal and ventral boundaries of the facial motor nucleus were identified in each rat by the large (up to 5 mV) negative antidromic field potential generated in the facial motor nucleus by stimulating the mandibular branch of the facial nerve (for details see Brown & Guyenet, 1985). Before starting the experiments, ventilation was adjusted to lower end-expiratory CO_2 – 4% at steady state (60–80 cycles s^{-1}; tidal volume 1–1.2 ml (100 g)$^{-1}$). These conditions were selected because 4% end-expiratory CO_2 was below the threshold of the PND. Variable amounts of pure CO_2 were then added to the breathing mixture to adjust end-expiratory CO_2 to the desired level.

All analog data (end-expiratory CO_2, sSND, lSND, PND, AP and unit activity) were stored on a microcomputer via a micro1401 digitizer from Cambridge Electronics Design (CED, Cambridge, UK) and were processed off-line using version 5 of the Spike 2 software (CED). Processing included action potential discrimination and binning, neuronal discharge rate measurement, and PND 'integration' (iPND) consisting of rectification and smoothing (τ, 0.015 s). Neural minute × volume (mvPND, a measure of the total phrenic nerve discharge per unit of time) was determined by averaging iPND over 50 s and normalizing the result by assigning a value of 0 to the dependent variable recorded at low levels of end-expiratory CO_2 (below threshold) and a value of 1 at the highest level of P_{CO_2} investigated (between 9.5 and 10%). The CED software was also used for acquisition of peri-event histograms of neuronal activity and peri-event averages of iPND. The peri-event histograms of neuronal single-unit activity were triggered on iPND trace and represented the summation of at least 100 respiratory cycles (350–800 action potentials per histogram).

The steady-state relationship between RVLM neuronal activity and end-expiratory CO_2 was obtained by stepping the inspired CO_2 level to various values for a minimum of 3 min and up to 5 min. The mean discharge rate of the neuron was measured during the last 30 s of each step at which time end-expiratory CO_2 and the discharge of the neuron appeared to have reached equilibrium. End-expiratory CO_2 was measured by averaging the maximum values recorded from 10 consecutive breaths at the midpoint of the time interval sampled.

Stimulation of carotid chemoreceptors was done with bolus injections of sodium cyanide (NaCN) (50 μg kg^{-1}, I.V.). Evidence that the stimulus activated brainstem neurons via stimulation of carotid chemoreceptors was obtained by demonstrating that denervation of these receptors eliminated the excitatory effect of the stimulus on PND.

Extracellular recording and juxtacellular labelling of neurons in the RVLM

Single-unit recording experiments were performed in seven baroreceptor-denervated halothane-anaesthetized rats, artificially ventilated rats. A concentric bipolar stimulating electrode was placed in the dorsolateral funiculus of the spinal cord at T2 for antidromic activation of RVLM neurons (Brown & Guyenet, 1985). The exposed surface of the spinal cord was immersed in warm mineral oil. The discharges of barosensitive neurons in the RVLM were recorded extracellularly as previously described (Schreihofer & Guyenet, 1997) using glass electrodes filled with 1.5% biotinamide (Molecular Probes, www.molecularprobes.com) in 0.5 M sodium acetate. Optimal electrode resistance for recording and labelling cells was 20–40 MΩ measured *in vivo*. Recordings were made with an intracellular amplifier in bridge mode (Axoclamp 2A, Axon Instruments, www.axon.com) to allow monitoring of action potentials during injection of current through the electrode. The RVLM was located using stereotaxic coordinates: 0–500 μm caudal to the caudal end of the facial nucleus (identified by the antidromic field potential), 1.6–2.0 mm lateral to the

midline, and 0–200 μm below the ventral extent of the facial field potential. The RVLM neurons selected for labelling had the following characteristics: proper location relative to the facial motor nucleus, spontaneous activity (18–20 Hz at rest) and antidromic activation from the spinal cord. As RVLM neurons generally exhibit a high level of spontaneous activity and are frequently subjected to medium-latency orthodromic excitation (> 8–10 ms), spontaneous collisions prevented identification of spinal-projecting axons except in neurons with fast-conducting spinal axons (latency < 8 ms). After electrophysiological characterization, RVLM bulbospinal neurons were filled with biotinamide using the previously described juxtacellular labelling method (200 ms pulses of 1.0–4.0 nA at 2.5 Hz for 1–3 min) (Schreihofer & Guyenet, 1997).

Intraparenchymal injections

Muscimol (Sigma; 1.75 mM in sterile saline pH 7.4) or kynurenic acid (Kyn) (Sigma; 50, 100 or 200 mM first dissolved in 1 N NaOH and then diluted in phosphate-buffered saline pH 7.4) was pressure injected (30–50 nl in 5 s) bilaterally through single-barrel glass pipettes (20 μm tip diameter). The solutions contained a 5% dilution of fluorescent latex microbeads (Lumafluor, New City, NY, USA) for later histological identification of the injection sites (Guyenet *et al.* 1990). The glass pipettes containing the drug–microbeads mixture also allowed recordings of field potentials and multiunit brain activity, properties that were used to help direct the electrode tip to the desired sites. Injections into RVLM were thus guided by recording the facial field potential and were placed 200 μm below the level corresponding to the lower edge of the field, 0–400 μm caudal to the caudal end of the field and 1.6–2.0 mm lateral to the midline. Injections into the RTN were also guided by recording the facial field potential and were placed 200 μm below the lower edge of the field, 1.6–1.9 mm lateral to the midline and 200–400 μm rostral to the caudal end of the field. Injections into the rostral ventral respiratory group (rVRG) were guided by locating inspiratory-related multiunit activity. The target region was found 500 μm rostral to the calamus scriptorius, 1.8 mm lateral to midline and 1.9–2.2 mm below the dorsal surface of the brainstem using electrodes angled 20 deg forward. The electrophysiological recordings were made on one side only and the second injection was placed 1–2 min later in the symmetric brain location (3.6 mm away) based on the stereotaxic coordinates of the first one. The classification of respiratory neurons was based on the timing of their discharge in relation to that of the phrenic nerve using accepted nomenclature (Feldman & McCrimmon, 1999). Injections into the commissural part of the nucleus of the solitary tract (commNTS) were made 400 mm caudal to the calamus scriptorius, in the midline and 0.3–0.5 mm below the dorsal surface of the brainstem.

Histology

At the end of the experiment the rat was deeply anaesthetized with halothane and perfused transcardially with PBS (pH 7.4) followed by paraformaldehyde (4% in 0.1 M phosphate buffer, pH 7.4). The brain was removed and stored in fixative for 24 h at 4°C. Using a vibrating microtome (Leica VT 1000S, Nussloch, Germany), 30 μm coronal sections were cut through the medulla and stored in a cryoprotectant solution at 20°C (Schreihofer & Guyenet, 1997). All histochemical procedures were done using free-floating sections according to previously described protocols. The sections were later processed for visualization of biotinamide and phenylethanolamine *N*-methyl transferase (PNMT) (Schreihofer & Guyenet, 1997). Biotinamide was revealed by incubating the sections in streptavidin conjugated with Alexa 488 (1 : 200; 3 h; Jackson Immunoresearch Laboratories, West Grove, PA, USA). This method was combined with immunofluorescent detection of PNMT using an already described rabbit polyclonal antibody (provided by M. C. Bohn) used at 1 : 2000 dilution and revealed with a Cy3-tagged anti-rabbit IgG (1 : 200; Jackson). Finally, the sections were mounted in sequential rostrocaudal order onto slides, dehydrated through a graded series of alcohol and xylene and covered with Krystalon (EMD Chemicals Inc, NJ, USA).

A conventional Zeiss Axioskop 2 multifunction microscope (brightfield, darkfield and epifluorescence) was used for all observations. Injection sites (fluorescent microbeads) and biotinamide-labelled neurons were plotted using a previously described computer-assisted mapping technique based on the use of a motor-driven microscope stage controlled by the Neurolucida software (Stornetta & Guyenet, 1999). The Neurolucida files were exported to the NeuroExplorer software (MicroBrightfield, Colchester, VT, USA) to count the various types of neuronal profiles within a defined area of the reticular formation.

Section alignment between brains was done relative to a reference section. To align sections around RVLM or RTN level, the most caudal section containing an identifiable cluster of facial motor neurons was identified in each brain and assigned the level 11.6 mm caudal to Bregma (Bregma −11.6 mm) according to the atlas of Paxinos & Watson (1998). Levels rostral or caudal to this reference section were determined by adding a distance corresponding to the interval between sections multiplied by the number of intervening sections. The same method was also used to identify the Bregma level of the muscimol injections targeted to the rVRG. When the object of the experiment was to locate injection sites at commissural NTS level, the

reference section used to align all others was the one closest to mid-area postrema level (Bregma −13.8 mm).

The Neurolucida files were exported to the Canvas 9 software drawing program for final modifications. Images were captured with a SensiCam QE 12-bit CCD camera (resolution 1376 × 1040 pixels, Cooke Corp., Auburn Hills, MI, USA). The neuroanatomical nomenclature is after Paxinos & Watson (1998).

Statistics

Statistical analysis was done with Sigma Stat version 3.0 (Jandel Corporation, Point Richmond, CA, USA). Data are reported as means ± standard error of the mean (S.E.M.). *t* test, paired *t* test and one-way parametric ANOVA followed by the Newman-Keul multiple comparisons test were used as appropriate. Significance was set at $P < 0.05$.

Results

Effect of central chemoreceptor stimulation on SND and PND

These experiments were performed in vagotomized, baro- and chemo-denervated rats (henceforth called completely denervated rats). PND and splanchnic SND (sSND) increased as a function of end-expiratory CO_2 and steady-state values were reached after about 3 min (Fig. 1*A*). Splanchnic SND exhibited its characteristic early inspiratory modulation (inset in Fig. 1*A*). The relationship between sSND and end-expiratory CO_2 at steady state was curvilinear suggesting the probable existence of a threshold around 4% CO_2 (Fig. 1*B*). The sSND response to CO_2 was anaesthetic-dependent and somewhat larger under halothane than urethane anaesthesia (Fig. 1*B*; steady-state SND increase from

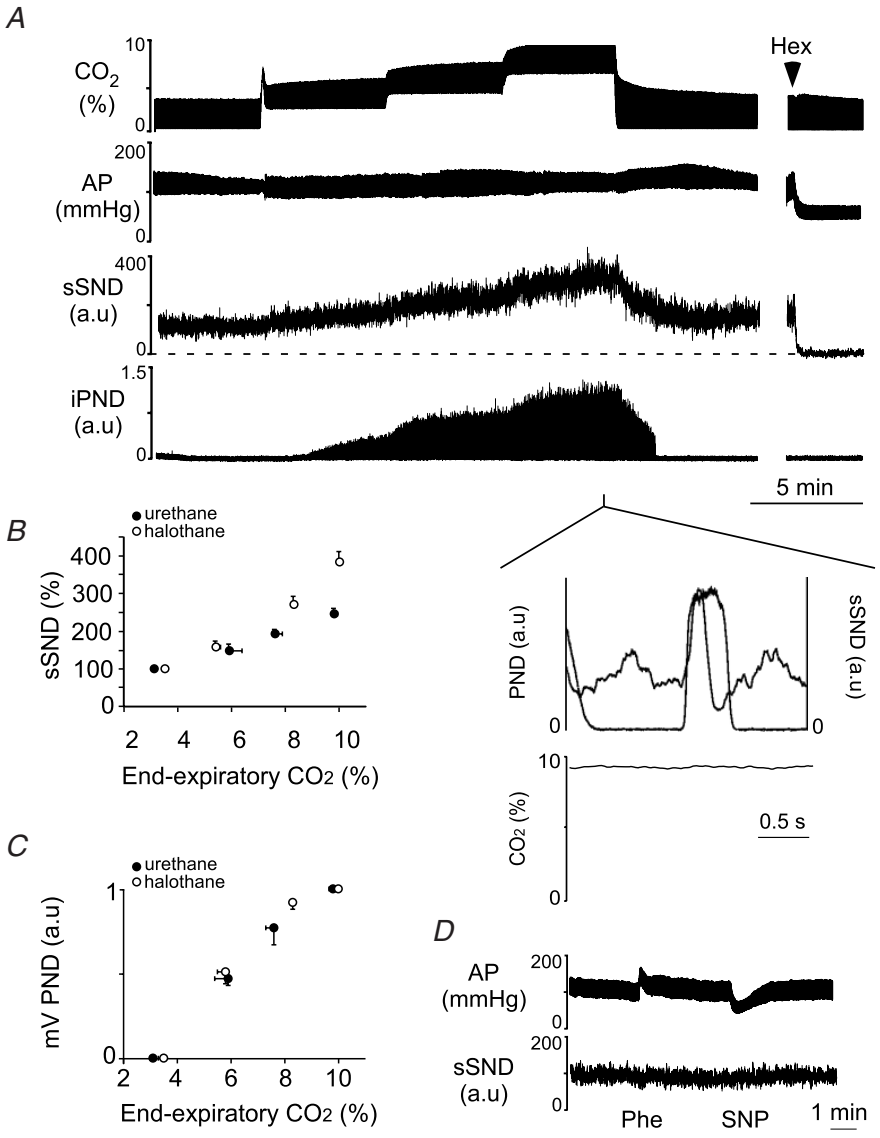

Figure 1. Effect of hypercapnia on SND and PND in vago-sino-aortic denervated rats
A, effect produced by step-wise increases in end-expiratory CO_2 on splanchnic SND (sSND) and PND in one rat. The ganglionic blocker hexamethonium (Hex) was used to define baseline SND. Inset shows the peri-event average of sSND triggered on the ascending phase of iPND. *B*, steady-state relationship between sSND and end-expiratory CO_2 under halothane (11 rats) or urethane anaesthesia (8 rats). sSND recorded at 3.3–3.8% CO_2 was defined as 100 units. The noise (0 unit) was defined by the hexamethonium method. *C*, steady-state relationship between mvPND (1 normalized unit equals the maximum value of the signal) and end-expiratory CO_2 for the rats shown in *B*. *D*, evidence that the animals were completely barodenervated (Phe, phenylephrine, 5 μg kg^{-1} I.V.; SNP, sodium nitroprusside 30 μg kg^{-1} I.V.).

Table 1. Effect of Kyn injection into RVLM on lumbar SND

	Low CO_2 (5%)	High CO_2 (10%)	Number of animals
Before Kyn	100	191 ± 3*	4
After Kyn	102 ± 4	193 ± 3*	4
Recovery	101 ± 2	189 ± 5*	4

Values are mean ± S.E.M. *Significantly different from rest (low CO_2). Kyn, kynurenic acid; SND, sympathetic nerve discharge.

3–3.5% to 9.5–10% CO_2: 388 ± 4% under halothane *versus* 250 ± 2% under urethane; $P < 0.05$). After normalization, the PND response to CO_2 was the same under both anaesthetics (Fig. 1*C*). The lack of response in sSND to acute changes in AP (Fig. 1*D*) and the absence of pulse synchrony in the sSND (data not shown) demonstrated that the preparation was baro-denervated. All animals showed complete denervation as indicated by one or both of these tests.

Lumbar SND (lSND) was recorded instead of splanchnic SND in four halothane-anaesthetized denervated rats. As expected, the respiratory modulation of lSND consisted of an early inspiratory depression, followed by a post-inspiratory peak (not illustrated; Haselton & Guyenet, 1989). Increasing end-expired CO_2 from 5% to 10% caused a 93% rise in lSND (Table 1). This increase was the same as that of the sSND when the latter was also measured while stepping end-expiratory CO_2 between 5 to 10% (97 ± 6%).

Effect of central chemoreceptor stimulation on the discharge rate of RVLM vasomotor neurons

Under anaesthesia, the baro-regulated class of sympathetic efferents is mainly controlled through sympathoexcitatory neurons located in the RVLM (Guyenet, 2006). The next experiments were designed to determine whether the

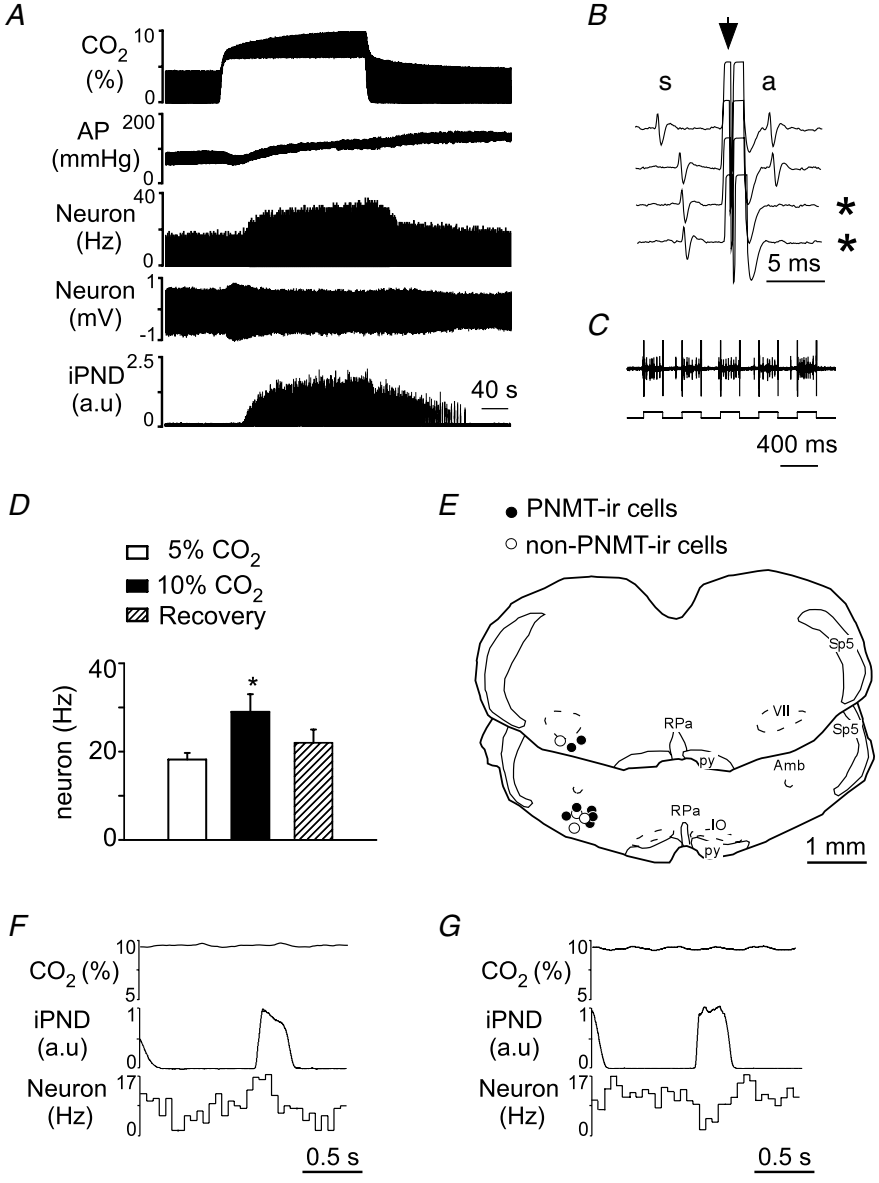

Figure 2. Effect of hypercapnia on the discharge rate of putative bulbospinal vasomotor neurons of the rostral ventrolateral medulla (RVLM) in vagotomized and sino-aortic deafferented rats
A, effect produced by stepping end-expiratory CO_2 from 5 to 10% on the discharge of a putative bulbospinal vasomotor neuron. *B*, time-controlled collision test showing that the neuron shown in *A* sends an axon to or through spinal segment T3 (* indicates two sweeps when collision occurred. Collisions (absence of the antidromic spike, a, were caused by decreasing the interval between a spontaneous spike, s, and the stimulus delivered to the spinal cord (arrow). *C*, procedure used to label the cell juxtacellularly with biotinamide (upper trace: unit; lower trace current monitor; 3.4 nA). *D*, mean effect of stepping CO_2 from 5 to 10% on 11 bulbospinal RVLM neurons (*$P < 0.05$ from both control and recovery values). *E*, location of the biotinamide-labelled neurons. The two coronal sections represent from top to bottom Bregma −11.6 and −11.8 mm after Paxinos & Watson (1998). *F*, PND-triggered activity histogram of the RVLM bulbospinal neuron shown in *A–C* reveals a respiratory pattern reminiscent of that of the splanchnic nerve. *G*, different RVLM neuron exhibiting a respiratory pattern reminiscent of that of the lumbar nerve. Amb, ambiguus nucleus; IO, inferior olive; py, pyramidal tract; RPa, raphe pallidus; sp5, spinal tract of trigeminal nerve; VII, facial motor nucleus.

sympathoexcitatory response to CO_2 is also associated with an increased activity of these RVLM neurons. Since the experiments had to be conducted in completely denervated rats, the identification of the bulbospinal sympathoexcitatory neurons located in the RVLM relied on criteria other than their barosensitivity namely location, spontaneous activity, axonal projection to the thoracic cord and respiratory modulation typical of lumbar or splanchnic SND. Cell location and cell phenotype (adrenergic or not) was determined following juxtacellular labelling (3.4 ± 0.2 nA for an average of 2 min). Eleven units with these characteristics were identified, labelled with biotinamide and recovered histologically (1–2 neurons per rat in 7 rats). Complete barodenervation was demonstrated by the lack of effects of raising or lowering AP on unit activity and the absence of a pulse modulation in the discharge of the cells (data not shown). Figure 2*A* shows the slowly developing activation of a putative sympathoexcitatory neuron. The collision test used to demonstrate that this cell had an axon at thoracic level is shown in Fig. 2*B*. The entrainment of the cell by extracellularly applied current (3.4 nA), which produces the uptake of biotinamide by the stimulated cell, is shown in Fig. 2*C* (upper trace, neuron; lower trace, juxtacellularly applied current). Every bulbospinal RVLM neuron tested was activated by hypercapnia. The average antidromic latency was 3.8 ± 0.6 ms (range: 3.1–7.8 ms). On average, increasing end-expired CO_2 from 5 to 10% raised the discharge rate of these cells from 18.2 ± 1.5 to 30 ± 3 spikes s^{-1} (67% increase; $P < 0.05$; Fig. 2*D*; range 20–130%). The increase in mean discharge rate was associated with an increase in AP of 25 ± 5 mmHg ($P < 0.05$; comparison between mean AP at rest and at the end of the hypercapnic episode). The unit shown in Fig. 2*A* had a respiratory modulation that was of central origin as indicated by the fact that ventilation and PND were asynchronous (flat PND-triggered end-expiratory CO_2 average, Fig. 2*F*). The peri-event activity histogram of this unit had an early inspiratory peak characteristic of splanchnic SND (Fig. 2*F*; compare with Fig. 1*A*, inset). This pattern was found in 4 of 11 units. Five units had the typical lumbar SND pattern (decreased firing probability during early inspiration and increased discharge during post-inspiration; Fig. 2*G*). The remaining two units had no obvious respiratory modulation. The location of the 11 biotinamide-labelled cells is shown in Fig. 2*E*. Seven neurons were PNMT-immunoreactive (Figs 2*E*, and 3*A* and *B*) and four were not (Figs 2*E*, and 3*C* and *D*). All the cells were found within the cluster of PNMT-ir neurons that defines the pressor region of the RVLM.

Effects of kynurenic acid injection into the rostral ventrolateral medulla on respiratory and sympathetic outflows

Most sympathoexcitatory reflexes are severely attenuated by blocking ionotropic excitatory amino acid (EAA) receptors in the RVLM (Guyenet, 2006). In order to test whether the sympathoactivation caused by stimulation of central chemoreceptors conforms to this general rule we injected the broad spectrum ionotropic EAA receptor antagonist kynurenic acid (Kyn) into the RVLM and tested the effect of this treatment on the rise in sSND and PND caused by stepping end-expiratory CO_2 from 5% to 10% for 5 min. Hypercapnia produced an immediate

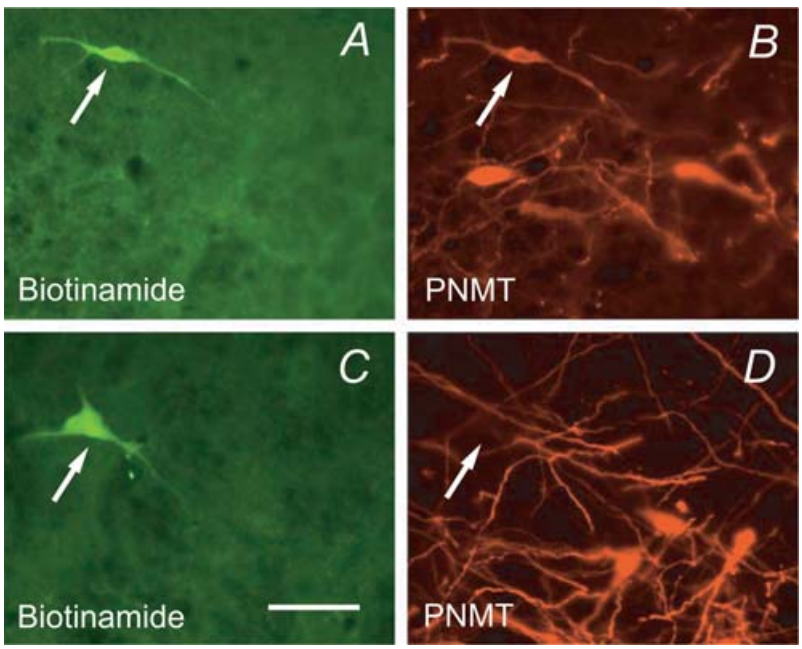

Figure 3. Phenotype of the recorded rostral ventrolateral medulla (RVLM) neurons
A and *B*, example of a biotinamide-labelled neuron that was immunoreactive for phenylethanolamine *N*-methyl transferase (PNMT, C1 adrenergic neuron). *C* and *D*, example of a recorded neuron that was negative for PNMT though located next to a cluster of C1 cells (calibration, 50 μm).

hypotension of -12 ± 8 mmHg followed 30 s later by a gradual return of AP to or slightly above control level. Immediately after return to 5% CO_2, AP increased by 23 ± 2 mmHg and returned to control values after 5 min.

Injections of Kyn (50 nl, concentration varying from 50 to 200 mM) were placed bilaterally in the RVLM of 18 totally denervated animals (50 mM in 6 rats, 100 mM in 5 rats and 200 mM in 7 rats). Kyn produced no effect on resting AP and sSND at any of the three doses. At 50 and 100 mM, Kyn reduced PND amplitude measured at 10% CO_2 by 54 and 72%, respectively, and increased the rate of the phrenic discharge (data not illustrated). At 200 mM, Kyn almost completely eliminated PND (Fig. 4*A* and *D*). Half-recovery time of PND ranged from 20 to 40 min and complete recovery from the effect of Kyn on PND occurred within 60 min (Fig. 4*D*). Kyn did not change the increase in sSND caused by hypercapnia at any of the three concentrations tested. The results produced by the highest dose of Kyn (200 mM) are illustrated in Fig. 4. Note that the drug changed neither the baseline value of sSND nor the level of sSND reached at steady state during hypercapnia (Fig. 4*A* and *B*). The hypercapnia-induced change in SND is replotted in Fig. 4*C* for clarity. The Kyn injection sites at the 200 mM dose ($N = 7$) are shown in Fig. 4*E*. These sites were centred on the region that contains the bulk of the bulbospinal sympathoexcitatory neurons of the RVLM (compare Figs 2*E* and 4*E*).

The surprising lack of effect of even the highest dose of Kyn on sSND response to CO_2 prompted us to verify that identical injections of Kyn could block the effect of peripheral chemoreceptor stimulation on sSND as described before (Koshiya *et al.* 1993; Sun & Reis, 1995). Bilateral injection of Kyn (50 nl, 200 mM into RVLM) in eight vagotomized urethane-anaesthetized rats with intact carotid sinus nerves did not change AP (118 ± 2.5 mmHg *versus* control, 121 ± 3 mmHg) or sSND at rest but these

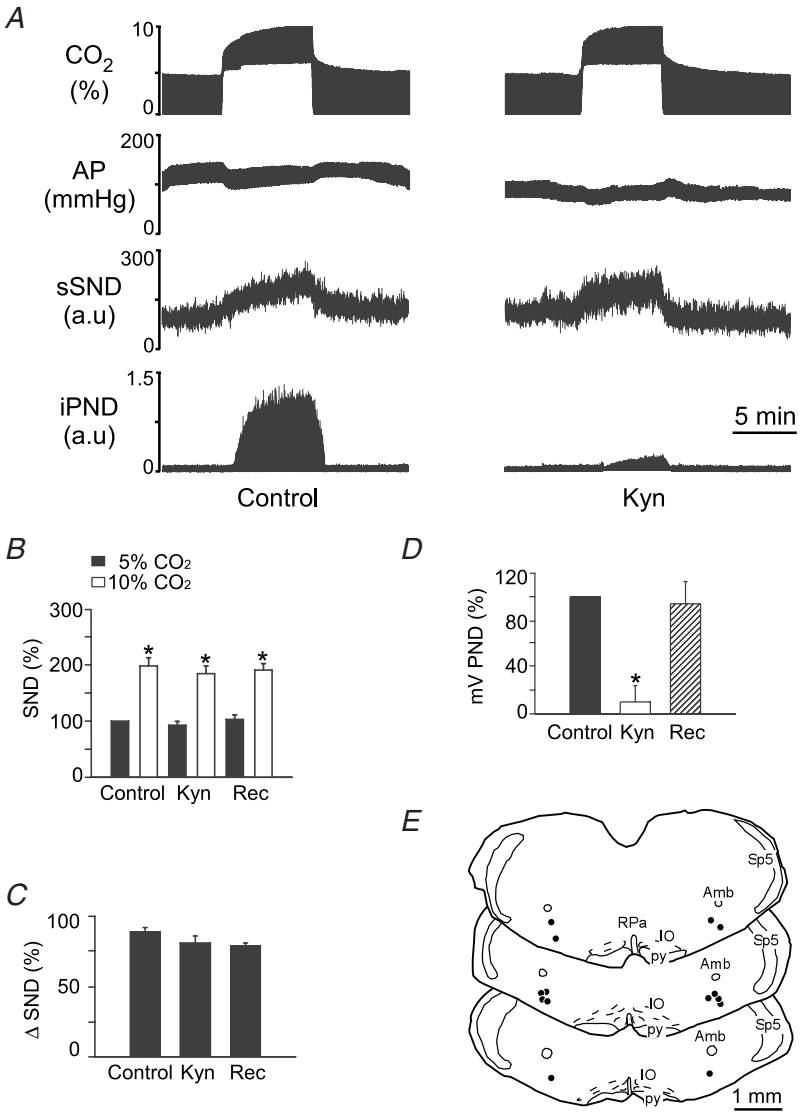

Figure 4. Kynurenic acid (Kyn) injection into the rostral ventrolateral medulla (RVLM) does not change the effect of hypercapnia on sSND in vagotomized sino-aortic deafferented rats
A, effect produced by stepping end-expiratory CO_2 from 5 to 10% on sSND and PND in one rat before and 5 min after bilateral microinjection of Kyn into RVLM (200 mM, 50 nl). *B*, average results from 7 rats. Resting sSND during the control period (5% CO_2) was defined as 100 units (*significant difference between 10 and 5% CO_2). Rec, recovery period (> 60 min after Kyn injection). *C*, effect produced by stepping end-expiratory CO_2 from 5 to 10% on sSND before, during and after Kyn (n.s.). *D*, effect of Kyn on mvPND elicited by stepping end-expiratory CO_2 from 5 to 10% ($^*P < 0.05$). *E*, injection sites. The three coronal sections represent from top to bottom Bregma −11.8, −11.96 and −12.3 mm after Paxinos & Watson (1998).

injections virtually eliminated resting PND and reduced by 86 ± 7% the increase in AP and sSND produced by I.V. injection of NaCN (Fig. 5*A* for representative case; Fig. 5*B* and *C* for average results).

Effects of bilateral injection of kynurenic acid into the retrotrapezoid nucleus on respiratory and sympathetic outflows

The RTN region contains chemosensitive neurons that probably provide an important source of excitatory drive to the respiratory network, especially under anaesthesia (Feldman *et al.* 2003). EAA receptor blockade in the RTN region has also been described as capable of decreasing the activity of the central respiratory pattern generator (Nattie & Li, 1995). The next experiments were therefore designed to determine whether bilateral blockade of EAA receptors in RTN can suppress the stimulatory effect of central chemoreceptor activation on PND and sSND. Kyn (200 mM, 50 nl) was injected bilaterally under electrophysiological guidance 200 μm below the facial motor nucleus and 200 μm rostral to the caudal end of this nucleus to target the region that contains the highest density of CO_2-sensitive RTN neurons according to our prior data (Mulkey *et al.* 2004; Guyenet *et al.* 2005*a*). Kyn reduced PND amplitude during hypercapnia by an average of 49% (Fig. 6*A* and *D*). Kyn also increased PND rate. However, the drug had no effect on the increase in sSND caused by increasing end-expiratory CO_2 from 5 to 10% (Fig. 6*B* and *C*). The effect of Kyn on PND was fully reversible within 60 min (Fig. 6*D*). Kyn injections did not change resting AP (control, 98 ± 4 mmHg; Kyn, 99 ± 5 mmHg). The Kyn injection sites were located below the caudal and medial edge of the facial motor nucleus (Fig. 6*E*). The fluorescent beads used to track the injection sites had spread approximately 240 μm on each side of the injection centre.

In brief, Kyn did not reduce the central stimulatory effect of hypercapnia on sSND, regardless of whether the injections were placed at the very rostral end of the RVLM, the region that includes the RTN (Fig. 6*E*), or slightly more caudally within the classically defined pressor region of RVLM (Fig. 4*E*). However, PND inhibition by Kyn was much greater when the drug was injected in the classically defined RVLM than when it was placed more rostrally into RTN (compare Figs 4*D* and 6*D*). This difference suggests that the VLM site at which Kyn inhibits respiration in our preparation is probably not the RTN but a region located caudal to it. This result is consistent with prior evidence that the discharge of RTN neurons is not affected by Kyn in our preparation (Mulkey *et al.* 2004). The difference between our results and those of Nattie & Li (1995) could be due to the fact that the carotid sinus nerves were cut in our preparation, thereby eliminating the glutamatergic excitatory input to the chemosensitive neurons of RTN (Takakura *et al.* 2006).

Effects of muscimol injection into the commissural portion of the solitary tract nucleus (commNTS) on respiratory and sympathetic chemoreflexes

The presence of acid-responsive neurons in the NTS and the fact that NTS acidification *in vivo* alters respiration has been interpreted as evidence that this structure contains central respiratory chemoreceptors (Nattie & Li, 2002; Feldman *et al.* 2003). The next experiments were designed to test the role played by commNTS in the activation of sSND and PND by increases in brain P_{CO_2}. This was accomplished by measuring the effects produced by microinjecting the $GABA_A$ receptor agonist muscimol (single 30 nl midline injection of 1.75 mM muscimol) into the commNTS of seven completely denervated halothane-anaesthetized rats. In order to verify our underlying assumption that muscimol did inhibit commNTS neurons we also examined the effect of similar injections on peripheral chemoreflexes. The latter experiments were

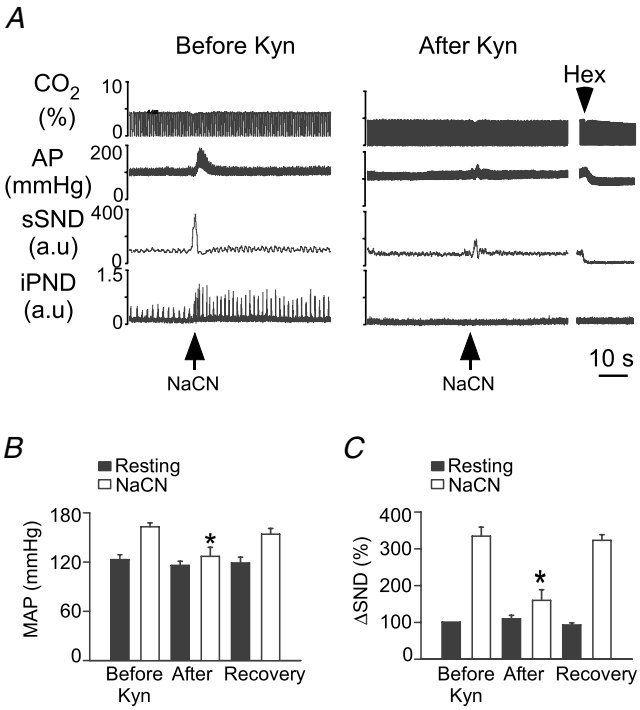

Figure 5. Kynurenic acid (Kyn) injection into rostral ventrolateral medulla (RVLM) greatly attenuate the peripheral chemoreflex in vagotomized rats

A, response of the splanchnic and phrenic nerves to peripheral chemoreceptor stimulation with I.V. cyanide (NaCN: 50 μg kg^{-1}) in a urethane-anaesthetized rat, before (left panel) and 5 min after bilateral injection of Kyn (200 mM, 50 nl: right panel) into RVLM. *B*, effect of Kyn on the cyanide-induced rise in MAP (*$P < 0.05$; 8 rats). *C*, effect of Kyn on the cyanide-induced rise in sSND (*$P < 0.05$; 8 rats).

conducted in eight vagotomized urethane-anaesthetized rats with intact carotid sinus nerves.

Muscimol had no effect on the sympathetic or the phrenic component of the central chemoreflex (representative example in Fig. 7*A*; summary data in Fig. 7*B* and *C*; histologically verified injection sites in Fig. 7*E*).

In vagotomized rats with intact carotid sinus nerves, muscimol injection into commNTS (7 rats) did not change resting PND but eliminated the activation of the sympathetic and respiratory outflows produced by stimulating the carotid bodies with NaCN (representative example in Fig. 8*A*; summary data in Fig. 8*B* and *C*). The muscimol injection sites (not illustrated) were indistinguishable from those shown in Fig. 7*E*.

Role of the caudal ventrolateral medulla in the central sympathetic chemoreflex

The rise in sympathetic vasomotor outflow elicited by central chemoreceptor stimulation is usually considered to be driven synaptically by the activation of the central respiratory pattern generator (Richter & Spyer, 1990). To test the validity of this assumption we examined whether pharmacological blockade of the central respiratory pattern generator alters the sympathetic response to hypercapnia in completely denervated rats. Pharmacological blockade of the respiratory network was performed by injecting drugs into the ventral respiratory columm caudal to the RVLM (also called CVLM). Kyn (200 mM, 50 nl per side) was used in a group of six completely denervated rats and muscimol (1.75 mM,

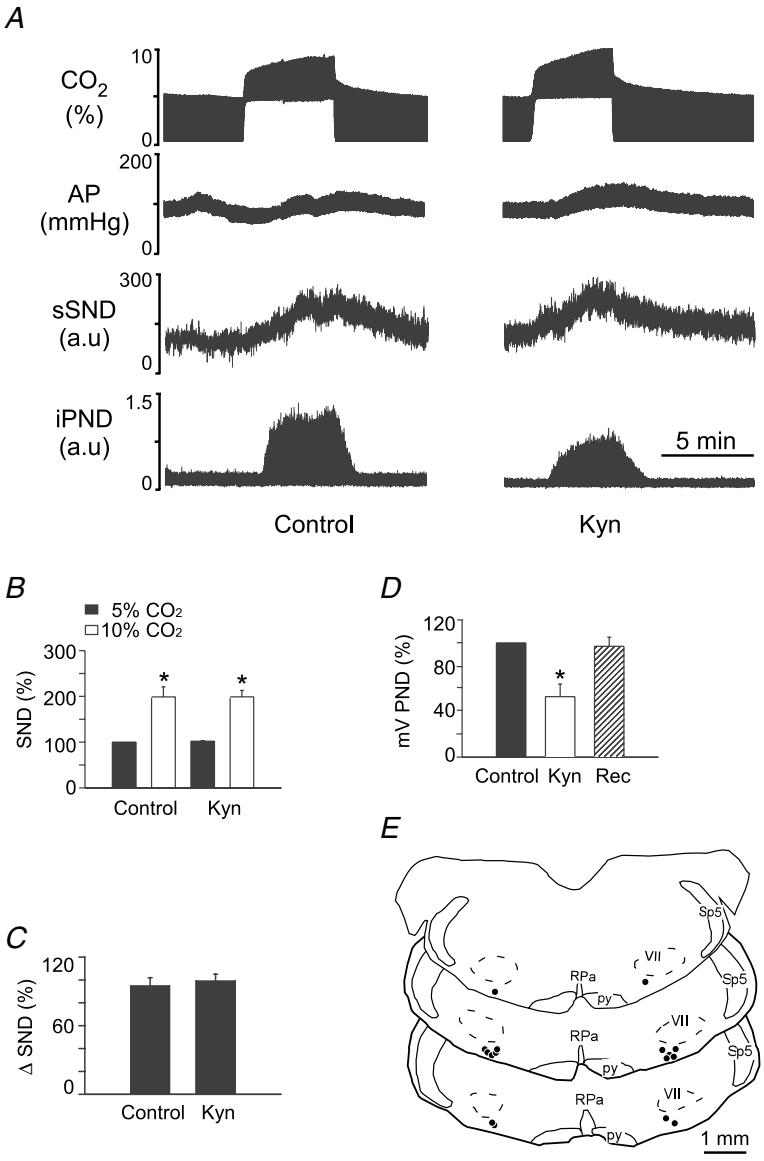

Figure 6. Kynurenic acid (Kyn) injection into the retrotrapezoid nucleus (RTN) does not change the effect of hypercapnia on sSND in vagotomized sino-aortic deafferented rats
A, effect produced by stepping end-expiratory CO_2 from 5 to 10% on sSND and PND in one rat before and after bilateral microinjection of Kyn into RTN (200 mM, 50 nl). *B*, average results from 8 rats. sSND at rest during the control period was defined as 100 units (*$P < 0.05$, significant difference between 10 and 5% CO_2). *C*, effect produced by stepping end-expiratory CO_2 from 5 to 10% on the CO_2-induced change in sSND before and 5 min after injection of Kyn (n.s.). *D*, effect of Kyn on mvPND elicited by stepping end-expiratory CO_2 from 5 to 10% (*$P < 0.05$ relative to control and recovery). *E*, injection sites. The three coronal sections represent from top to bottom Bregma −11.0, −11.3 and −11.6 mm after Paxinos & Watson (1998).

30 nl per side) was used in a second group of rats ($n = 9$). The injections were placed under electrophysiological guidance into a region of the rVRG/CVLM where strong inspiratory-related multiunit activity could be recorded from the injection pipette. The effects of these injections on the respiratory system were gauged by their effect on PND.

Kyn injection into the CVLM eliminated PND for up to 60 min and prevented its activation by CO_2 (Fig. 9*A* and *D*). The injection centres were located close to 1.5 mm posterior to the caudal end of the facial motor nucleus (Fig. 9*E*). By our previous estimates, these sites correspond to the CVLM and the rostral end of the rVRG (Stornetta *et al.* 2003). The fluorescent microbeads extended 250 ± 12 μm on each side of the injection centre and therefore Kyn, which diffuses more freely that microbeads, is likely to have also reached the respiratory neurons located in the pre-Bötzinger complex. Bilateral injection of Kyn increased resting AP from 100 ± 3 to 132 ± 5 mmHg ($P < 0.05$) and resting sSND from 100 to 125% ($P < 0.05$). Kyn also significantly increased the effect of hypercapnia on sSND (Fig. 9*B* and *C*).

Virtually identical results were obtained when muscimol instead of Kyn was injected into CVLM (8 rats; example in Fig. 10*A*; summary data in Fig. 10*B*–*D*; injection sites in Fig. 10*E*). Note that muscimol increased resting AP from 103 ± 2 to 139 ± 5 mmHg ($P < 0.05$), eliminated PND, increased resting sSND to 148 ± 9% of control level ($P < 0.05$) and increased the magnitude of the sympathetic nerve response to central chemoreceptor stimulation (Fig. 10*C*).

Discussion

The present study indicates that the sympathoactivation caused by rises in brain P_{CO_2} is predominantly mediated

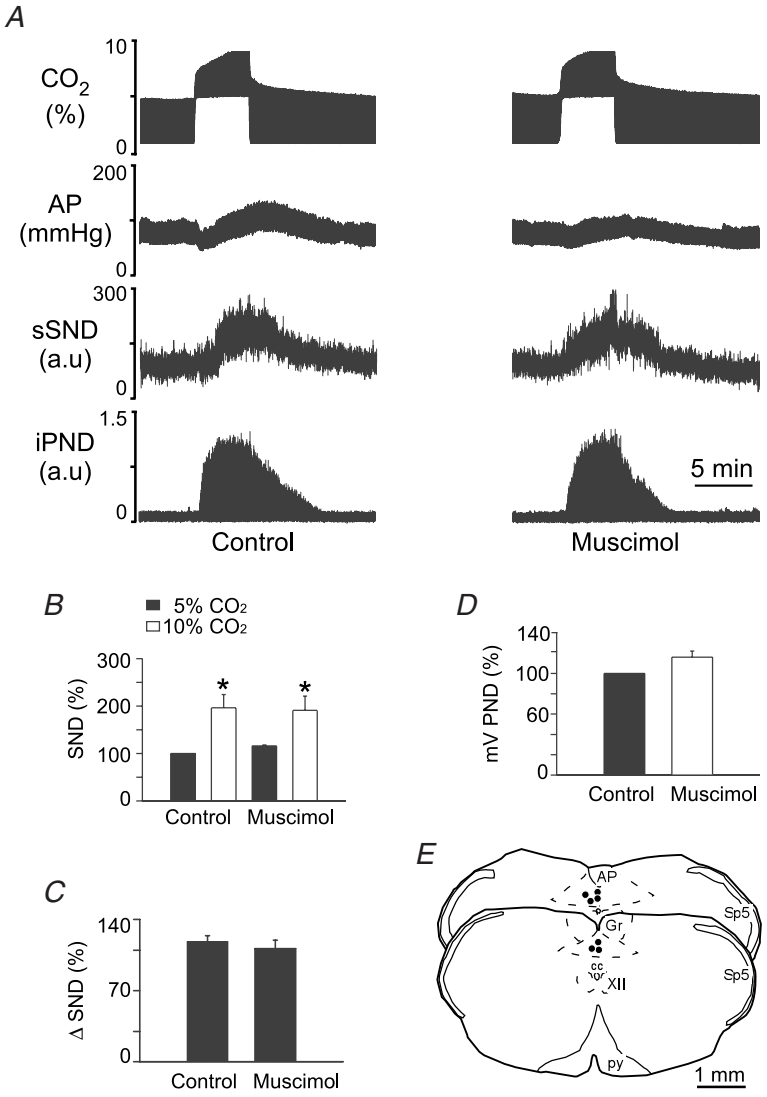

Figure 7. Muscimol injection into the commissural part of the solitary tract nucleus (commNTS) does not change the effect of hypercapnia on sSND or PND in vagotomized sino-aortic denervated rats
A, effect produced by stepping end-expiratory CO_2 from 5 to 10% on sSND and PND in one rat before and after a single midline microinjection of muscimol into commNTS (1.75 mM, 30 nl). *B*, average results from 7 rats. sSND at rest during the control period was defined as 100 units (*$P < 0.05$ between 10 and 5% CO_2). *C*, effect produced of stepping end-expiratory CO_2 from 5 to 10% on the CO_2-induced increase in sSND before and 5 min after injection of muscimol (n.s.). *D*, effect of muscimol on mvPND elicited by stepping end-expiratory CO_2 from 5 to 10% (n.s.). *E*, injection sites. The two coronal sections represent from top to bottom Bregma −14.08 and −14.3 mm after Paxinos & Watson (1998). AP, area postrema; cc, central canal; Gr, gracile nucleus; XII, hypoglossal nucleus; for other abbreviations see Fig. 2.

by the activation of C1 and other sympathoexcitatory neurons of the RVLM. We also show that the activation of these neurons does not rely on chemoreceptors located within the commNTS or the rVRG-pre-Bötzinger region (CVLM). Finally, we also show that hypercapnia activates an inhibitory input to RVLM neurons, which reduces the overall effect of CO_2 on the sympathetic outflow. These results and the pertinent literature are discussed in the context of the largely novel scheme depicted in Fig. 11. An essential aspect of the proposed scheme is that the excitatory effect of CO_2 on RVLM sympathoexcitatory neurons results either from the intrinsic chemosensitivity of these cells or from the activation of the pH-sensitive interneurons located in RTN. The second essential feature of the scheme is that the respiratory modulation of SND is attributed to two processes: active inhibition by GABAergic neurons located in CVLM and disfacilitation of the RTN neurons. The respiratory modulation of the sympathoexcitatory neurons is viewed as attenuating the overall activation of the sympathetic outflow caused by elevations of central nervous system (CNS) P_{CO_2}.

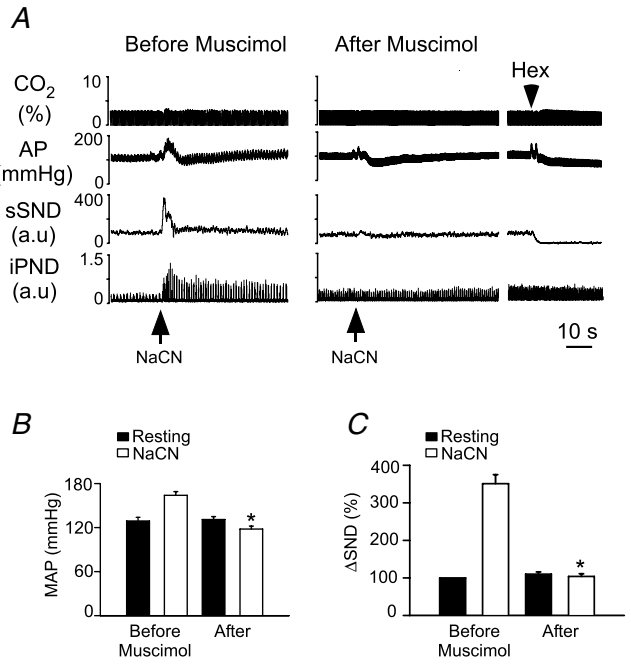

Figure 8. Muscimol injection into commissural part of the solitary tract nucleus (commNTS) blocks peripheral chemoreflexes in vagotomized rats
A, response of the splanchnic and phrenic nerves to peripheral chemoreceptor stimulation with I.V. cyanide (50 μg kg^{-1}) in a urethane-anaesthetized rat before (left panel) and 5 min after a single midline injection of muscimol (1.75 mM, 30 nl: right panel) into commNTS. *B*, effect of muscimol on the cyanide-induced rise in MAP (*$P < 0.05$ when comparing effect of NaCN before and after muscimol; 7 rats). *C*, effect of muscimol on the cyanide-induced rise in sSND (*$P < 0.05$; 7 rats).

RVLM sympathoexcitatory neurons contribute to the sympathoactivation caused by central chemoreceptor stimulation

Under anaesthesia, hypercapnia markedly increases sympathetic efferent activity in vagotomized and sino-aortic denervated preparations (Preiss & Polosa, 1977; Hanna *et al.* 1981; Millhorn & Eldridge, 1986). In agreement with this well-established phenomenon, the mass activity of the splanchnic or lumbar nerves almost doubled at steady state in our preparation when end-expiratory CO_2 was raised from 5 to 10% and SND more than tripled relative to the baseline recorded at 3.5% CO_2. The type of respiratory entrainment observed in these sympathetic nerves during central chemoreceptor stimulation (early inspiratory peak in splanchnic and post-inspiratory peak in lumbar) also conformed to prior observations in rats (Numao *et al.* 1987; Darnall & Guyenet, 1990; Guyenet *et al.* 1990; Pilowsky *et al.* 1996). As shown before, the magnitude of the respiratory modulation of SND (difference between apex and nadir) is less pronounced in rats than in other species and its pattern is also different. In our experimental preparation, virtually all the activity recorded in these nerves is silenced by stimulating arterial baroreceptors (Haselton & Guyenet, 1989) therefore the recorded activity consists overwhelmingly of baroregulated vasoconstrictor efferents (Guyenet, 2006).

In our experiments hypercapnia produced an almost immediate hypotension, which most probably results from a direct (i.e. not sympathetically mediated) effect of CO_2 on the vasculature and, possibly, on cardiac contractility. Blood pressure gradually came back up during hypercapnia to reach about control level at the end of the episode. Then, just after the hypercapnia episode, BP tended to overshoot briefly. We assume that this overshoot reflects the increase in sympathetic activity at a time when the direct depressant effect of CO_2 on the vasculature was rapidly waning.

The effect of central chemoreceptor stimulation on the activity of RVLM vasomotor neurons has rarely been examined before, presumably because of the difficulty in identifying these neurons in a preparation in which arterial baroreceptors have been cut. The only prior attempt (Haselton & Guyenet, 1989) reported a mean increase in discharge of 36 ± 8% between 5 and 10% end-expiratory CO_2. The present result is 67 ± 4%. The difference is probably due to the fact that we measured the effect of CO_2 at steady state (3–5 min equilibration) in the present experiments whereas the cells were exposed to shorter periods of hypercapnia in our prior study. As shown by the kinetics of the phrenic response, several minutes are required for equilibration. This delay is required to establish a steady state in brain pH and medullary blood flow (Sato *et al.* 1992). The difference may

also be related to the selection of neurons. In the present study, our sample consisted exclusively of neurons with fast-conducting axons in which the collision test could be performed. Medium latency (8–25 ms) orthodromic spikes evoked by spinal cord stimulation collide systematically with antidromic spikes in slow-conducting bulbospinal sympathoexcitatory RVLM neurons, preventing the identification of their spinal axon. Seven of the 11 recorded cells were PNMT-immunoreactive, which is consistent with the previously described properties of fast-conducting barosensitive sympathoexcitatory neurons of the RVLM (Schreihofer & Guyenet, 1997). In the present case we do not know with certainty that the presumed sympathoexcitatory neurons that we recorded would have been regulated by arterial baroreceptors but this is very likely because, in our previous experience, all spontaneously active bulbospinal neurons located in the rostral C1 region are inhibited by raising AP in animals with intact baroreceptor afferents. In any event, the essential point in the present context is that the recorded neurons were identified as sympathoexcitatory neurons. This is unquestionably the case for the seven bulbospinal adrenergic cells that were recorded because such C1 cells are known to innervate sympathetic preganglionic neurons and probably the case of the other four bulbospinal neurons although the level of evidence is less persuasive in this case (for review see Guyenet, 2006).

It is of course impossible to be sure that a 67% increase in the activity of RVLM neurons fully accounts for a 97% increase in vasomotor SND. This uncertainty is compounded by the fact that we could not identify neurons with slowly conducting axon velocity in the present study. In other words, the present data do not exclude the possibility that other neurons (e.g. A5) might contribute to the SND increase caused by central chemoreceptor stimulation.

In preparations with intact baroreceptors and carotid bodies, the activation of RVLM vasomotor neurons by hypercapnia is of more modest amplitude (Haselton & Guyenet, 1989). In some cases, no significant change has been reported at the population level (McAllen, 1987; Mulkey *et al.* 2004). Possible explanations include the heterogeneity of the bulbospinal sympathoexcitatory neurons and, again, the fact that the hypercapnic stimulus might have been of too short duration. The more likely explanation perhaps is that the changes in RVLM neuron activity produced by increasing central P_{CO_2} are attenuated by baroreceptor feedback due to the rise in AP, especially

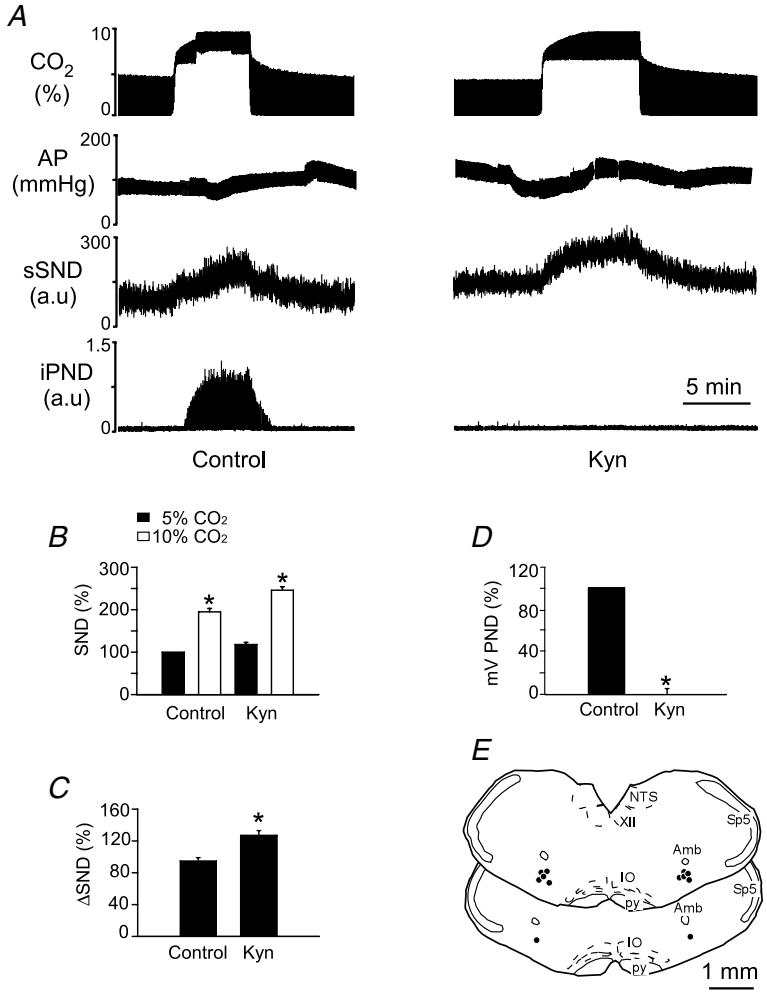

Figure 9. Kynurenic acid (Kyn) injection into the caudal ventrolateral medulla (CVLM) increases the effect of hypercapnia on sSND in vagotomized sino-aortic deafferented rats
A, effect produced by stepping end-expiratory CO_2 from 5 to 10% on sSND and PND in one rat before and after bilateral microinjection of Kyn into CVLM (200 mM, 50 nl). *B*, average results from 6 rats. sSND at rest during the control period was defined as 100 units (*$P < 0.05$ between 10 and 5% CO_2). *C*, effect produced by stepping end-expiratory CO_2 from 5 to 10% on sSND before and after injection of Kyn into CVLM (*$P < 0.05$). *D*, effect of Kyn on mvPND elicited by stepping end-expiratory CO_2 from 5 to 10% (*$P < 0.05$ between control and drug). *E*, injection sites. The two coronal sections represent from top to bottom Bregma −13.3 and −13.6 mm after Paxinos & Watson (1998). NTS, nucleus of the solitary tract; for other abbreviations see Fig. 2.

in those neurons that have the most powerful input from these receptors and are thus the easiest to identify. This attenuation may be further accentuated by the fact that the baroreceptor feedback to the vasomotor SND is more potent under conditions that increase the activity of the central respiratory pattern generator (Chruscielewski *et al.* 1975; Trzebski & Kubin, 1981; Miyawaki *et al.* 1995). This potentiation can probably be explained by the integrative properties of the CVLM neurons that mediate the baroreflex as will be discussed below and is illustrated in Fig. 11.

The chemoreceptors located in the solitary tract and the rVRG-pre-Bötzinger region do not contribute to the sympathoactivation caused by increasing brain P_{CO_2}

Central respiratory chemoreceptors are neurons that directly or indirectly detect changes in CNS interstitial fluid pH and ultimately influence the respiratory network. Such neurons have been tentatively identified in many lower brainstem regions, including the NTS, the medullary raphe and several regions of the ventrolateral medulla including the pre-Bötzinger region and the retrotrapezoid nucleus (Guyenet *et al.* 2005*b*; Nattie & Li, 2006). Whether the same or different chemoreceptors are implicated in the central effect of CO_2 on the sympathetic outflow is an unsettled question. The lack of effect of muscimol injection into commNTS indicates that the caudal cardiorespiratory portion of the NTS plays no role in the sympathoexcitatory response to central chemoreceptor stimulation under the anaesthetic conditions that we selected. The elimination of the peripheral chemoreflex caused by such injections in rats with intact carotid nerves demonstrated how effective muscimol was at inhibiting commNTS neurons. Yet, acidification of commNTS via microdialysis of CO_2-enriched fluid does increase respiration in awake

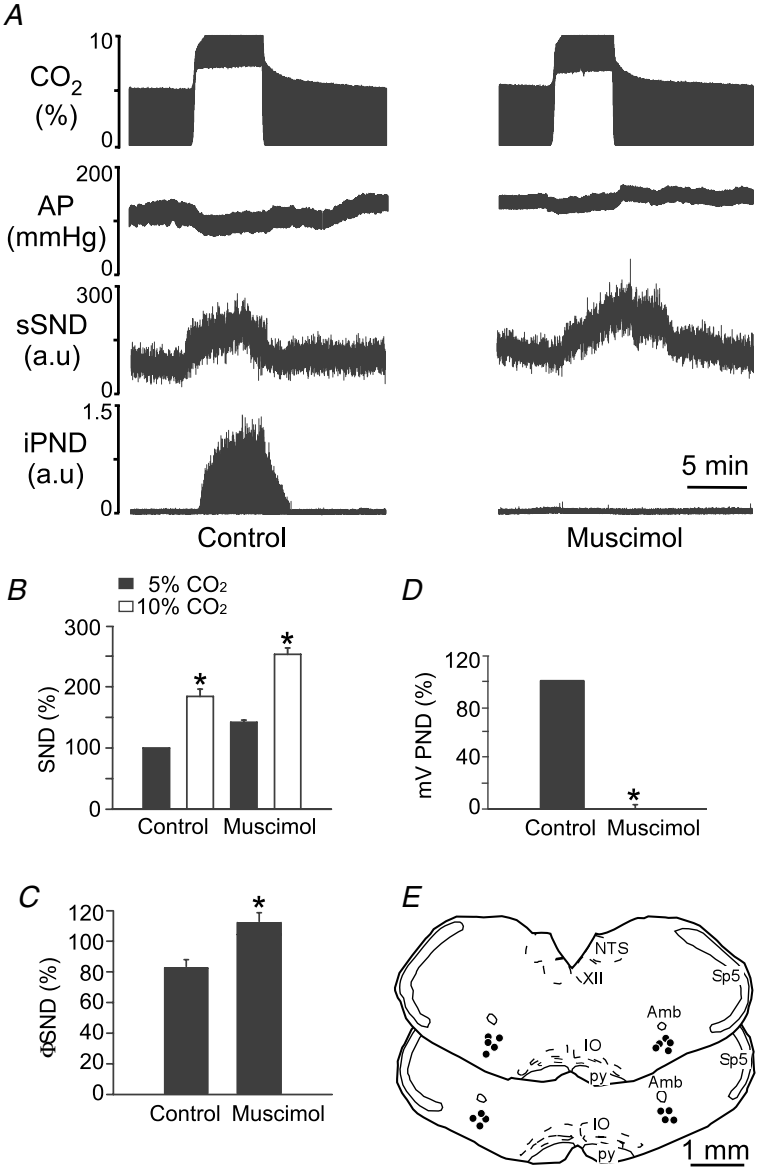

Figure 10. Muscimol injection into the caudal ventrolateral medulla (CVLM) increases the effect of hypercapnia on sSND in vagotomized sino-aortic deafferented rats
A, effect produced by stepping end-expiratory CO_2 from 5 to 10% on sSND and PND in one rat before and after bilateral microinjection of muscimol into CVLM (1.75 mM, 30 nl). *B*, average results from 9 rats. sSND at rest during the control period was defined as 100 units (*$P < 0.05$ for effect of hypercapnia relative to baseline). *C*, effect produced of stepping end-expiratory CO_2 from 5 to 10% on sSND before and 5 min after injection of muscimol into CVLM (*$P < 0.05$ for effect of muscimol). *D*, effect of muscimol on mvPND elicited by stepping end-expiratory CO_2 from 5 to 10% (*$P < 0.05$). *E*, injection sites. The two coronal sections represent from top to bottom Bregma −13.3 and −13.6 mm after Paxinos & Watson (1998).

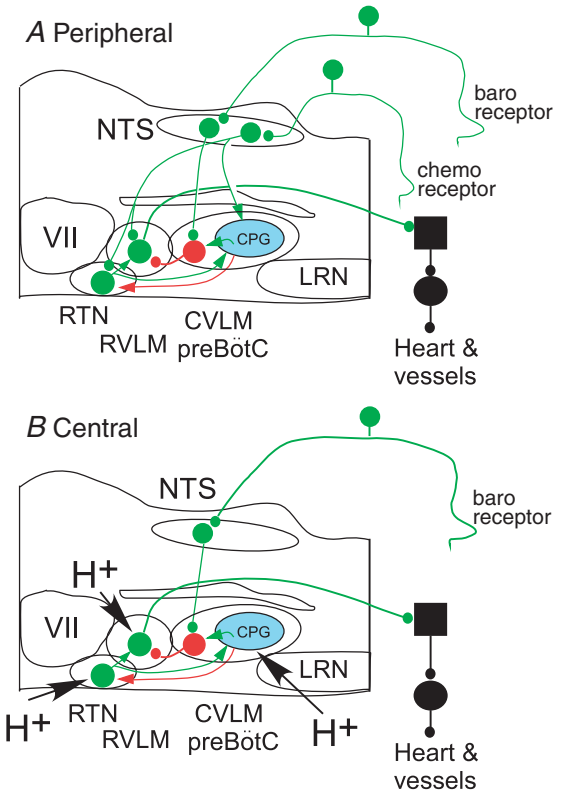

Figure 11. Working model of the sympathetic chemoreflexes
A, peripheral chemoreflex. The increased SND is mediated primarily by activation of the bulbospinal sympathoexcitatory neurons of the RVLM. The excitatory drive of RVLM neurons operates via a direct glutamatergic input from commNTS neurons and via a di-synaptic input that relays via the intrinsically chemosensitive neurons of RTN. The latter pathway is therefore modulated by the degree of central chemoreceptor stimulation. The respiratory modulation of SND and RVLM neurons is seen as deriving from two mechanisms, respiratory-phasic activation by the CPG (respiratory rhythm and pattern-generating network, in blue) of the GABAergic neurons that mediate the sympathetic baroreflex (neuron in red) and respiratory-phasic inhibition of RTN neurons (red arrow, transmitter unidentified). The first mechanism causes an active inhibition of RVLM neurons and the second causes a disfacilitation of RVLM neurons via reduction in RTN discharges. In combination, these two processes attenuate the activation of RVLM neurons during chemoreceptor stimulation and cause the respiratory modulation of SND. *B*, central chemoreflex. The increased SND caused by raising CNS P_{CO_2} is driven via activation of the bulbospinal sympathoexcitatory neurons of the RVLM. The relevant chemoreceptors are located in the RVLM region. The activation of RVLM neurons by extracellular fluid acidification is mediated synaptically via the chemosensitive neurons of RTN and, possibly, by the intrinsic chemosensitivity of the RVLM sympathoexcitatory neurons. The respiratory modulation of RVLM neurons and SND has the same mechanism as in the case of the peripheral chemoreflex (CPG-mediated activation of the CVLM neurons and CPG-mediated inhibition of the RTN). CNS acidification activates the CPG via chemoreceptors located in the RTN and/or the rVRG-pre-Bötzinger region but not in the NTS. The integrative properties of the CVLM GABAergic neurons that relay the sympathetic baroreflex (in red) account for the well-documented potentiation of the baroreflex caused by increasing CPG activity. The scheme only applies to the effect of chemoreceptors on the baroregulated sympathetic efferents that control the heart and resistance vessels. The scheme is not applicable to other sympathetic efferents (e.g. to skin or brown adipose fat). Excitatory neurons in green (large circles, cell bodies; small circles, ionotropic glutamatergic synapses; green arrows, neurochemically uncharacterized excitatory connections). In red, GABAergic CVLM neurons involved in the sympathetic baroreflex. Red arrow, neurochemically unidentified inhibitory input from the CPG to RTN neurons. CPG, central pattern generator; CVLM, caudal ventrolateral medulla; LRN, lateral reticular nucleus; RTN, retrotrapezoid nucleus; RVLM, rostral ventrolateral nucleus; for other abbreviations see Fig. 2.

rats (Nattie & Li, 2002). The discrepancy can be explained three ways. The first explanation, improbable perhaps but impossible to exclude, is that artificial acidification via microdialysis of CO_2 or with acetazolamide does not mimic the effect of systemic hypercapnia. Second, anaesthesia may eliminate the effect produced by acidifying the NTS. Third, the pH-sensitive cells of the NTS (central chemoreceptors) reside in a different location than the second-order cells involved in the peripheral chemoreflex. In support of this view, the NTS region acidified by Nattie & Li (2002) with resulting stimulation of breathing was slightly more rostral and lateral than that which we targeted with muscimol in the present study.

The rVRG-pre-Bötzinger region of the ventral respiratory column also contains putative respiratory chemoreceptors (Solomon *et al.* 2000; Nattie & Li, 2006). These receptors are apparently not involved in the sympathoexcitation caused by hypercapnia since bilateral injection of muscimol or Kyn into this region did not decrease the effect of CO_2 on SND. Kyn, which only blocks EAA transmission, could conceivably have spared the chemoreceptors responsible for activating RVLM neurons but this explanation does not hold in the case of muscimol, a $GABA_A$ receptor agonist that silences all neurons. The neuronal inhibition caused by muscimol was profound given the hours-long disappearance of the PND at rest and during hypercapnia. Inhibition of the rVRG-pre-Bötzinger region with either Kyn or muscimol actually increased the sympathoexcitation caused by hypercapnia, suggesting that this region contains an inhibitory input to RVLM neurons that is activated by CNS acidification.

Putative organization of the medullary network responsible for peripheral and central sympathetic chemoreflexes

The following discussion is an attempt to fit the results of the present study and the pertinent literature into a novel and more comprehensive theory of how the sympathetic vasomotor outflow is regulated by central and peripheral chemoreceptors. In this scheme, the increase in SND caused by central or peripheral chemoreceptor stimulation is seen as resulting from excitatory drives to RVLM neurons. The scheme incorporates the already established notion that RVLM neurons are excited by

peripheral chemoreceptors via a direct glutamatergic input from commNTS (for review and references see Guyenet, 2000). To this notion, we add the concept that this glutamatergic projection also activates RVLM neurons via a di-synaptic excitatory pathway from commNTS to RVLM that relays via the chemosensitive neurons of the retrotrapezoid nucleus (RTN; secondary input) (Fig. 11*A*) (Takakura *et al.* 2006). In the case of the central chemoreflex (Fig. 11*B*) the primary excitatory input to RVLM neurons is seen as originating from the chemosensitive neurons of RTN although the possibility that the RVLM sympathoexcitatory neurons might be intrinsically sensitive to pH is also considered (Fig. 11*B*). The respiratory entrainment of RVLM neurons and SND, which is a feature common to both reflexes, is viewed as being mediated by the following two mechanisms: respiratory synchronous inhibitory inputs to RVLM neurons originating from the GABAergic neurons of the CVLM, that normally mediate the baroreflex, and respiratory-synchronous disfacilitation caused by respiratory-synchronous inhibitory inputs to RTN neurons (Fig. 11*A* and *B*).

The GABAergic cells of the CVLM are respiratory-modulated and many have a phase-spanning respiratory modulation that mirrors that of the sympathoexcitatory neurons of the RVLM (Mandel & Schreihofer, 2006). Such characteristics are therefore consistent with the possibility that these neurons contribute to the respiratory entrainment of RVLM neurons. Inhibition of CVLM neurons by muscimol should thus increase the central sympathetic chemoreflex, as observed in the present experiments. CVLM blockade should also increase the peripheral chemoreflex and eliminate its respiratory oscillations, as observed in prior experiments (Koshiya & Guyenet, 1996).

The proposed scheme is also consistent with prior observation that the RTN chemosensitive neurons have a phase-spanning type of respiratory modulation in rats (Guyenet *et al.* 2005*a*). Like CVLM neurons, RTN cells are heterogeneous with regard to respiratory modulation but cases of respiratory patterns that are identical to those of RVLM sympathoexcitatory neurons (early inspiratory or post-inspiratory peak) have been found, consistent with the possibility that these particular RTN neurons drive RVLM sympathoexcitatory neurons (Guyenet *et al.* 2005*a*). Furthermore, in cats, species in which RVLM neurons and the vasomotor SND are inspiratory modulated, the predominant respiratory pattern of RTN neurons is also inspiratory (Connelly *et al.* 1990). The respiratory entrainment of RTN neurons is most probably due to respiratory-phasic inhibitory inputs (Guyenet *et al.* 2005*a*). Phasic inhibition of these chemosensitive neurons by the central respiratory network should therefore attenuate the chemoreflexes by a process of disfacilitation. We have already demonstrated that respiratory-rhythmic inhibition of RTN neurons disappears after injection of muscimol into the CVLM region whereas the excitatory response of these neurons to central and peripheral chemoreceptor stimulation persists (Guyenet *et al.* 2005*a*). Therefore, by silencing the respiratory pattern generator, muscimol inhibition of the CVLM region should also eliminate the respiratory modulation of RTN neurons and this effect should also contribute to increasing the magnitude of the sympathetic chemoreflex, as was observed.

The present study revealed that the excitatory mechanisms responsible for the central and the peripheral chemoreflex are distinct in one essential respect. Ionotropic glutamatergic receptor blockade in RVLM virtually eliminates SND activation by peripheral chemoreceptors whereas it does not attenuate the central sympathetic chemoreflex (present study). The effect of Kyn on the peripheral chemoreflex is consistent with prior anatomical and electrophysiological evidence that the effect of peripheral chemoreceptor activation is transmitted to RVLM and RTN neurons by a direct glutamatergic projection from commNTS (Sun & Reis, 1995; Aicher *et al.* 1996; Guyenet, 2000; Takakura *et al.* 2006). This fact accounts for the very large attenuation of the peripheral chemoreflex by Kyn injection into RVLM (86% in the present case) since such injections should block the direct activation of the sympathoexcitatory neurons and their indirect activation via the RTN neurons.

The resistance of the central sympathetic chemoreflex to Kyn indicates that the activation of the RVLM neurons does not involve ionotropic glutamate receptors. This observation suggests two alternative possibilities represented in Fig. 11*B*. The effect of CO_2 on RVLM neurons could result from the intrinsic chemosensitivity of these neurons or it could be caused by synaptic inputs from chemosensitive cells that do not operate via ionotropic glutamate receptors. The notion that RVLM neurons might be intrinsically pH-sensitive still rests on extremely circumstantial evidence outlined in the introduction but it cannot be dismissed *a priori*. The presence within the RVLM region of central chemoreceptors that activate the sympathoexcitatory neurons synaptically is much more plausible however, and the RTN neurons have all the required characteristics. Briefly summarized, RTN neurons are activated by pH, they are located at the rostral end of the RVLM at the ventral surface and they are in close proximity to the sympathoexcitatory neurons (Guyenet *et al.* 2005*b*). Their activation by CO_2 is independent of ionotropic glutamate transmission and their discharge pattern becomes extremely regular after inhibition of the CPG (Mulkey *et al.* 2004; Takakura *et al.* 2006). These cells innervate the region of the RVLM (Rosin *et al.* 2006) and, as mentioned above, a fraction of RTN neurons have the same phase-spanning respiratory modulation (early inspiratory

or post-inspiratory) as the sympathoexcitatory neurons of the RVLM (Guyenet *et al.* 2005*a*). The inability of Kyn to attenuate the central sympathetic chemoreflex (this study) might seem to exclude RTN neurons *a priori* because these cells express VGLUT2 and therefore should release glutamate (Mulkey *et al.* 2004). However, RTN neurons may operate via metabotropic glutamate receptors or they could release other excitatory transmitters. Metabotropic glutamate receptors may be present on RVLM neurons given that agonists of these receptors increase AP substantially when they are injected into RVLM (Tsuchihashi *et al.* 2000). The literature contains many examples of VGLUT2-expressing CNS neurons that release another transmitter that appears to play the dominant role in synaptic transmission, e.g. orexin neurons (Rosin *et al.* 2003).

In summary, the hypothetical scheme presented in Fig. 11 could account satisfactorily for most if not all existing observations. However, its accuracy will have to be subjected to further and far more detailed testing.

References

Aicher SA, Saravay RH, Cravo S, Jeske I, Morrison SF, Reis DJ & Milner TA (1996). Monosynaptic projections from the nucleus tractus solitarii to C1 adrenergic neurons in the rostral ventrolateral medulla: Comparison with input from the caudal ventrolateral medulla. *J Comp Neurol* **373**, 62–75.

Brown DL & Guyenet PG (1985). Electrophysiological study of cardiovascular neurons in the rostral ventrolateral medulla in rats. *Circ Res* **56**, 359–369.

Chruscielewski L, Majcherczyk S & Trzebski A (1975). Influence of combined baro- and chemoreceptor stimulation upon sympathetic activity. *J Physiol* **247**, 28*P*–29*P*.

Connelly CA, Ellenberger HH & Feldman JL (1990). Respiratory activity in retrotrapezoid nucleus in cat. *Am J Physiol Lung Cell Mol Physiol* **258**, L33–L44.

Darnall RA & Guyenet P (1990). Respiratory modulation of pre- and postganglionic lumbar vasomotor sympathetic neurons in the rat. *Neurosci Lett* **119**, 148–152.

Feldman JL & McCrimmon DR (1999). Neural control of breathing. In *Fundamental Neuroscience*, ed.Zigmond MJ, Bloom FE, Landis SC, Roberts JL & Squire LR, pp. 1063–1090. Academic Press, San Diego.

Feldman JL, Mitchell GS & Nattie EE (2003). Breathing: rhythmicity, plasticity, chemosensitivity. *Annu Rev Neurosci* **26**, 239–266.

Guyenet PG (2000). Neural structures that mediate sympatho-excitation during hypoxia. *Respir Physiol* **121**, 147–162.

Guyenet PG (2006). The sympathetic control of blood pressure. *Nat Rev Neurosci* **7**, 335–346.

Guyenet PG, Darnall RA & Riley TA (1990). Rostral ventrolateral medulla and sympathorespiratory integration in rats. *Am J Physiol Regul Integr Comp Physiol* **259**, R1063–R1074.

Guyenet PG & Koshiya N (1992). Respiratory-sympathetic integration in the medulla oblongata. In *Central Neural Mechanisms in Cardiovascular Regulation*, Vol. II, ed. Kunos G & Ciriello J, pp. 226–247. Birkhauser, Boston.

Guyenet PG, Mulkey DK, Stornetta RL & Bayliss DA (2005*a*). Regulation of ventral surface chemoreceptors by the central respiratory pattern generator. *J Neurosci* **25**, 8938–8947.

Guyenet PG, Stornetta RL, Bayliss DA & Mulkey DK (2005*b*). Retrotrapezoid nucleus: a litmus test for the identification of central chemoreceptors. *Exp Physiol* **90**, 247–253.

Habler HJ, Janig W & Michaelis M (1994). Respiratory modulation in the activity of sympathetic neurones. *Prog Neurobiol* **43**, 567–606.

Hanna BD, Lioy F & Polosa C (1979). The effect of cold blockade of the medullary chemoreceptors on the CO_2 modulation of vascular tone and heart rate. *Can J Physiol Pharmacol* **57**, 461–468.

Hanna BD, Lioy F & Polosa C (1981). Role of carotid and central chemoreceptors in the CO_2 response of sympathetic preganglionic neurons. *J Auton Nerv Syst* **3**, 421–435.

Hanna BD, Lioy F & Polosa C (1988). Role of carotid and central chemoreceptors in the CO2 response of sympathetic preganglionic neurons. *J Auton Nerv Syst* **3**, 95–105.

Haselton JR & Guyenet PG (1989). Central respiratory modulation of medullary sympathoexcitatory neurons in rat. *Am J Physiol Regul Integr Comp Physiol* **256**, R739–R750.

Hodges MR, Martino P, Davis S, Opansky C, Pan LG & Forster HV (2004). Effects on breathing of focal acidosis at multiple medullary raphe sites in awake goats. *J Appl Physiol* **97**, 2303–2309.

Koshiya N, Huangfu D & Guyenet PG (1993). Ventrolateral medulla and sympathetic chemoreflex in the rat. *Brain Res 23* **609**, 174–184.

Koshiya N & Guyenet PG (1996). Tonic sympathetic chemoreflex after blockade of respiratory rhythmogenesis in the rat. *J Physiol* **491**, 859–869.

McAllen RM (1987). Central respiratory modulation of subretrofacial bulbospinal neurons in the cat. *J Physiol* **388**, 533–545.

Mandel DA & Schreihofer AM (2006). Central respiratory modulation of barosensitive neurones in rat caudal ventrolateral medulla. *J Physiol* **572**, 881–896.

Millhorn DE (1986). Neural respiratory and circulatory interaction during chemoreceptor stimulation and cooling of ventral medulla in cats. *J Physiol* **370**, 217–231.

Millhorn DE & Eldridge FL (1986). Role of ventrolateral medulla in regulation of respiratory and cardiovascular systems. *J Appl Physiol* **61**, 1249–1263.

Milner TA, Pickel VM, Morrison SF & Reis DJ (1989). Adrenergic neurons in the rostral ventrolateral medulla: ultrastructure and synaptic relations with other transmitter-identified neurons. *Prog Brain Res* **81**, 29–47.

Milner TA, Pickel VM, Park DH, Joh TH & Reis DJ (1987). Phenylethanolamine N-methyltransferase-containing neurons in the rostral ventrolateral medulla of the rat. I. Normal ultrastructure. *Brain Res* **411**, 28–45.

Miyawaki T, Pilowsky P, Sun QJ, Minson J, Suzuki S, Arnolda L, Llewellyn-Smith I & Chalmers J (1995). Central inspiration increases barosensitivity of neurons in rat rostral ventrolateral medulla. *Am J Physiol Regul Integr Comp Physiol* **268**, R909–R918.

Mulkey DK, Stornetta RL, Weston MC, Simmons JR, Parker A, Bayliss DA & Guyenet PG (2004). Respiratory control by ventral surface chemoreceptor neurons in rats. *Nat Neurosci* **7**, 1360–1369.

Nattie EE & Li A (1995). Rat retrotrapezoid nucleus iono- and metabotropic glutamate receptors and the control of breathing. *J Appl Physiol* **78**, 153–163.

Nattie EE & Li A (1996). Central chemoreception in the region of the ventral respiratory group in the rat. *J Appl Physiol* **81**, 1987–1995.

Nattie EE & Li AH (2002). CO_2 dialysis in nucleus tractus solitarius region of rat increases ventilation in sleep and wakefulness. *J Appl Physiol* **92**, 2119–2130.

Nattie E & Li A (2006). Central chemoreception 2005: a brief review. *Auton Neurosci* **126–127**, 332–338.

Numao Y, Koshiya N, Gilbey MP & Spyer KM (1987). Central respiratory drive-related activity in sympathetic nerves of the rat: the regional differences. *Neurosci Lett* **81**, 279–284.

Paxinos G & Watson C (1998). *The Rat Brain in Stereotaxic Coordinates*, 4th edn. Academic Press, San Diego.

Pilowsky P, Arnolda L, Chalmers J, Llewellyn-Smith I, Minson J, Miyawaki T & Sun QJ (1996). Respiratory inputs to central cardiovascular neurons. *Ann NY Acad Sci* **783**, 64–70.

Pineda J & Aghajanian GK (1997). Carbon dioxide regulates the tonic activity of locus coeruleus neurons by modulating a proton- and polyamine-sensitive inward rectifier potassium current. *Neurosci* **77**, 723–743.

Preiss G & Polosa C (1977). The relation between end-tidal CO_2 and discharge patterns of sympathetic preganglionic neurons. *Brain Res* **122**, 255–267.

Putnam RW, Filosa JA & Ritucci NA (2004). Cellular mechanisms involved in CO_2 and acid signaling in chemosensitive neurons. *Am J Physiol Cell Physiol* **287**, C1493–C1526.

Richerson GB, Wang W, Hodges MR, Dohle CI & Diez-Sampedro A (2005). Homing in on the specific phenotype(s) of central respiratory chemoreceptors. *Exp Physiol* **90**, 259–266.

Richter DW & Spyer KM (1990). Cardiorespiratory control. In *Central Regulation of Autonomic Functions*, ed. Loewy AD & Spyer KM, pp. 189–207. Oxford University Press, New York.

Rosin DL, Chang DA & Guyenet PG (2006). Afferent and efferent connections of the rat retrotrapezoid nucleus. *J Comp Neurol* **499**, 64–89.

Rosin DL, Weston MC, Sevigny CP, Stornetta RL & Guyenet PG (2003). Hypothalamic orexin (hypocretin) neurons express vesicular glutamate transporters VGLUT1 or VGLUT2. *J Comp Neurol* **465**, 593–603.

Sato A, Trzebski A & Zhou W (1992). Local cerebral blood flow responses in rats to hypercapnia and hypoxia in the rostral ventrolateral medulla and in the cortex. *J Auton Nerv Syst* **41**, 79–86.

Schreihofer AM & Guyenet PG (1997). Identification of C1 presympathetic neurons in rat rostral ventrolateral medulla by juxtacellular labeling in vivo. *J Comp Neurol* **387**, 524–536.

Schreihofer AM & Guyenet PG (2000*a*). Role of presympathetic C1 neurons in the sympatholytic and hypotensive effects of clonidine in rats. *Am J Physiol Regul Integr Comp Physiol* **279**: R1753–R1762.

Schreihofer AM & Guyenet PG (2000*b*). Sympathetic reflexes after depletion of bulbospinal catecholaminergic neurons with anti-DbetaH-saporin. *Am J Physiol Regul Integr Comp Physiol* **279**, R729–R742.

Schreihofer AM, Stornetta RL & Guyenet PG (2000). Regulation of sympathetic tone and arterial pressure by rostral ventrolateral medulla after depletion of C1 cells in rat. *J Physiol*; **529**, 221–236.

Schreihofer AM & Guyenet PG (2003). Baroactivated neurons with pulse-modulated activity in the rat caudal ventrolateral medulla express GAD67 mRNA. *J Neurophysiol* **89**, 1265–1277.

Solomon IC, Edelman NH & O'Neill MH (2000). CO_2/H^+ chemoreception in the cat pre-Bötzinger complex in vivo. *J Appl Physiol* **88**, 1996–2007.

Stornetta RL & Guyenet PG (1999). Distribution of glutamic acid decarboxylase mRNA-containing neurons in rat medulla projecting to thoracic spinal cord in relation to monoaminergic brainstem neurons. *J Comp Neurol* **407**, 367–380.

Stornetta RL, Sevigny CP & Guyenet PG (2003). Inspiratory augmenting bulbospinal neurons express both glutamatergic and enkephalinergic phenotypes. *J Comp Neurol* **455**, 113–124.

Sun QJ, Goodchild AK & Pilowsky PM (2001). Firing patterns of pre-Botzinger and Botzinger neurons during hypocapnia in the adult rat. *Brain Res* **903**, 198–206.

Sun M-K & Reis DJ (1995). NMDA receptor-mediated sympathetic chemoreflex excitation of RVL-spinal vasomotor neurones in rats. *J Physiol* **482**, 53–68.

Takakura AC, Moreira TS, Colombari E, West GH, Stornetta RL & Guyenet PG (2006). Peripheral chemoreceptor inputs to retrotrapezoid nucleus (RTN) CO_2-sensitive neurons in rats. *J Physio1* **572**, 503–523.

Trzebski A & Kubin L (1981). Is the central inspiratory activity responsible for pCO_2-dependent drive of the sympathetic discharge? *J Auton Nerv Syst* **3**, 401–420.

Tsuchihashi T, Liu Y, Kagiyama S, Matsumura K, Abe I & Fujishima M (2000). Metabotropic glutamate receptor subtypes involved in cardiovascular regulation in the rostral ventrolateral medulla of rats. *Brain Res Bull* **52**, 279–283.

Washburn CP, Bayliss DA & Guyenet PG (2003). Cardiorespiratory neurons of the rat ventrolateral medulla contain TASK-1 and TASK-3 channel mRNA. *Respir Physiol Neurobiol* **138**, 19–35.

Acknowledgements

This research was supported by grants from the National Institutes of Health to P.G.G. (HL 28785) and Coordenação de Aperfeiçoamento de Pessoal de Nível Superior to T.S.M. (BEX 3495/04-3) and to A.C.T. (BEX 4402/05-7).